Acetonitrile synthesis via ammoxidation: Mo/zeolites catalysts screening

Faouzi Ayari[a*], Emna Mannei[a,b], Esther Asedegbega–Nieto[c], Mourad Mhamdi[b,d], Gérard Delahay[e]

[a] University of Monastir, Faculty de Pharmacy of Monastir, Laboratory of chemical, galenic and pharmacological development of drugs, 5000 Monastir, Tunisia
[b] University of Tunis El Manar, Faculty of Sciences of Tunis, Material chemistry and catalysis laboratory, Tunis El Manar, 2092 Tunis, Tunisia
[c] The National Distance Education University (UNED), Faculty of Sciences, Department of inorganic and technical chemistry, 28040 Madrid, Spain
[d] University of Tunis El Manar, Higher institute of medical technologies of Tunis, 1006 Tunis, Tunisia
[e] Charles Gerhardt Institute in Montpellier, CNRS–UM–ENSCM–MACS, 34296 Montpellier Cedex 05, France

[*] Corresponding author. Tel.: +21650646504.
E-mail address: faouzi.ayari@fst.utm.tn
ORCID ID: orcid.org/0000-0003-0684-424X

Catalysts characterization and catalytic tests

The chemical analyses were performed by ICP (Optima 3300 DV Perkin Elmer spectrometer) and EDX (JEOL–JEM 2100F instrument, X–MAX detector, accelerating voltage of 200 kV and energy resolution of 20 eV). Nitrogen physisorption at –196 °C was carried out with an automatic ASAP 2020 apparatus (Micromeritics) after dehydration at 250°C overnight. BET model was used to calculate the specific surface area (S_{BET}), while *t*–plot method was employed to determine the external surface area and micropore volume (V_{micro}). However, the porous volume (V_p) was calculated at the end of the step corresponding to the filling of the pores (at P/P° = 0.98). XRD features were collected from a Siemens D–500 diffractometer throughout the 2θ range of 2–70°. TEM and SEM images were collected from a JEOL JEM–2000 FX and a HITACHI 4800 S electron microscope, respectively. H_2–TPR analysis was performed on an Autochem II 2920 V3.05 analyzer with H_2/He flow (30 cm^3 min^{-1}) and 70 mg of sample. NH_3–TPD analysis was carried out with the same H_2–TPR equipment. The sample was first exposed to an air flow then saturated with flowing NH_3 at 100 °C and flushed with helium at the same temperature. Finally, the temperature was ramped to 550 °C (10 °C min^{-1}). XPS analyses were performed with an OMICRON photoelectron spectrometer using the magnesium as anode. The deconvolution of each spectrum was made using Casa XPS software. DRIFTS spectra were recorded on a Bruker IFS 55 spectrometer equipped with a Thermo Spectra Tech reacting cell. UV/Vis DRS analysis was performed with a Perkin Elmer Lambda 45 spectrophotometer using $BaSO_4$ as reference material.

A series of catalytic tests was carried out using m = 200 mg of catalyst and the following gas composition: 10 % of C_2H_6, 10 % of NH_3 and 10 % of O_2. The total flow rate was maintained at 100 cm^3 min^{-1} by balancing with helium (contact time = 0.08 *s*). Another series of runs was performed for ethylene ammoxidation using m = 50 mg of catalyst (0.02 *s*) and the same gas composition. The mass of catalyst as well as the total flow rate were carefully optimized in order to avoid internal and external diffusions. The outlet gases were analyzed by two chromatographic units (flame ionization and thermal conductivity detectors). During ammoxidation, insignificant amounts of CO, CH_4 and NO were also produced and they were not included in the calculations.

The conversion (Eq. 1), selectivity (Eq. 2) and activity (Eq. 3) were defined as follow:

Conversion of hydrocarbon H (C_2H_6 or C_2H_4): $$X_H = \frac{\sum_i y_i n_i}{y_H n_H + \sum_i y_i n_i} \times 100 \qquad (1)$$

i = AN, C_2H_4 and CO_2 (for H = C_2H_6) and *i* = AN and CO_2 (for H = C_2H_4).

Selectivity of product P_i (*i* = AN, C_2H_4 and CO_2): $$S_i = \frac{y_i n_i}{\sum_i y_i n_i} \times 100 \qquad (2)$$

Here, y_i and y_H are the mole fractions of product P_i (AN, C_2H_4 and CO_2) and reactant H, respectively, while n_i and n_H are the number of carbon atoms in each molecule of product P_i and reactant H, respectively.

Activity of product P_i : $$Ac_i(\text{mol } s^{-1}g^{-1}) = \frac{\text{Hydrocarbon flow } (\text{cm}^3\, s^{-1}) \times X_H \times S_i}{\text{Molar volume (STP, cm}^3\text{mol}^{-1}) \times 10^4 \times \text{m (g)}} \qquad (3)$$

The turnover frequency (TOF), *i.e.* the activity per each Mo specie molecule:

$$\text{TOF } (s^{-1}) = \frac{Ac_i \text{ (mol } s^{-1}g^{-1})}{\text{Amount of Mo specie by gram of sample (mol g}^{-1})} \qquad (4)$$

Table S1: List of the prepared solids

No	Sample	Zeolite	Provider	Precursor	Provider
I	Mo–OFF	H^+–OFF	–	$MoCl_3$	Merck
II	Mo–FER	NH_4^+–FER	Zeolyst	$MoCl_3$	Merck
III	Z26($MoCl_3$)	NH_4^+–ZSM-5	Zeolyst CBV5524G	$MoCl_3$	Merck
IV	Z15($MoCl_3$)	H^+–ZSM-5	Zeolyst CBV3024E	$MoCl_3$	Merck
V	MOR($MoCl_3$)	NH_4^+–MOR	Zeolyst CBV21A	$MoCl_3$	Merck
VI	BEA($MoCl_3$)	NH_4^+–BEA	Zeolyst CP814E	$MoCl_3$	Merck
VII	Z26($MoOCl_4$)	NH_4^+–ZSM-5	Zeolyst CBV5524G	$MoOCl_4$	Sigma–Aldrich
VIII	Z26($MoCl_5$)	NH_4^+–ZSM-5	Zeolyst CBV5524G	$MoCl_5$	Alfa Aesar
IX	Z26(MoCO)	NH_4^+–ZSM-5	Zeolyst CBV5524G	$Mo(CO)_6$	Aldrich Chem Co.
X	Z26(MoAcac)	NH_4^+–ZSM-5	Zeolyst CBV5524G	$MoO_2(C_5H_7O_2)_2$	Merck Schuchardt
XI	Z26(MoO_3)6%He	NH_4^+–ZSM-5	Zeolyst CBV5524G	MoO_3	Merck Schuchardt
XII	BEA(MoO_3)	NH_4^+–BEA	Zeolyst CP814E	MoO_3	Merck Schuchardt
XIII	BEA(MoAcac)	NH_4^+–BEA	Zeolyst CP814E	$MoO_2(C_5H_7O_2)_2$	Merck Schuchardt
XIV	BEA(MoCO)	NH_4^+–BEA	Zeolyst CP814E	$Mo(CO)_6$	Aldrich Chem Co.
XV	BEA($MoCl_5$)	NH_4^+–BEA	Zeolyst CP814E	$MoCl_5$	Alfa Aesar
XVI	BEA($MoOCl_4$)	NH_4^+–BEA	Zeolyst CP814E	$MoOCl_4$	Sigma–Aldrich
XVII	BEA(Mo_7O_{24})	NH_4^+–BEA	Zeolyst CP814E	$(NH_4)_6Mo_7O_{24}\cdot 4H_2O$	Merck Schuchardt
XVIII	Z26(MoO_3)10%He	NH_4^+–ZSM-5	Zeolyst CBV5524G	MoO_3	Merck Schuchardt
XIX	Z140(MoO_3)6%He	NH_4^+–ZSM-5	Zeolyst (CBV28014)	MoO_3	Merck Schuchardt
XX	Z15(MoO_3)Imp2%	H^+–ZSM-5	Zeolyst CBV3024E	MoO_3	Merck Schuchardt
XXI	Z15(MoO_3)Imp4%	H^+–ZSM-5	Zeolyst CBV3024E	MoO_3	Merck Schuchardt
XXII	Z40(MoO_3)Imp2%	H^+–ZSM-5	Zeolyst (CBV8014)	MoO_3	Merck Schuchardt
XXIII	Z40(MoO_3)Imp4%	H^+–ZSM-5	Zeolyst (CBV8014)	MoO_3	Merck Schuchardt
XXIV	**Z26(MoO_3)6%O_2**	**NH_4^+–ZSM-5**	**Zeolyst CBV5524G**	**MoO_3**	**Merck Schuchardt**
XXV	**Z140(MoO_3)6%He**	**NH_4^+–ZSM-5**	**Zeolyst (CBV28014)**	**MoO_3**	**Merck Schuchardt**

Table S2: Catalytic behaviour of Mo containing solids in C_2H_6 ammoxidation at different temperatures

No	Catalyst	X (%)	S (%)			Ac_{CH_3CN} (μmol $s^{-1}g^{-1}$)	$Ac_{C_2H_4}$ (μmol s^{-1} g^{-1})
			CH_3CN	C_2H_4	CO_2		
I	Mo–OFF	6 (500°C)	3	5	92	0.10	0.10
II	Mo–FER	– (500°C)	–	–	–	–	–
III	Z26($MoCl_3$)	7 (500°C)	49	9	42	1.30	0.20
		5 (475°C)	13	5	82	0.24	0.11
		4 (450°C)	9	3	89	0.13	0.04
		4 (425°C)	7	2	91	0.10	0.03
IV	Z15($MoCl_3$)	6 (500°C)	35	10	55	0.80	0.20
		5 (475°C)	18	6	76	0.33	0.11
		5 (450°C)	11	2	87	0.20	0.04
		4 (425°C)	8	1	91	0.12	0.01
V	MOR($MoCl_3$)	6 (500°C)	4	8	88	0.10	0.20
		6 (475°C)	3	4	93	0.07	0.09
		6 (450°C)	3	2	95	0.07	0.04
		6 (425°C)	2	1	97	0.04	0.02
VI	BEA($MoCl_3$)	7 (500°C)	15	17	68	0.40	0.40
		6 (475°C)	13	8	79	0.29	0.18
		6 (450°C)	10	5	85	0.22	0.11
		4 (425°C)	11	2	87	0.16	0.03
VII	Z26($MoOCl_4$)	4 (500°C)	20	10	70	0.30	0.15
		4 (475°C)	19	6	75	0.28	0.09
		4 (450°C)	12	4	84	0.18	0.06
		4 (425°C)	8	2	90	0.12	0.03
VIII	Z26($MoCl_5$)	9 (500°C)	85	9	6	3.00	0.30
		6 (475°C)	83	7	10	1.85	0.16
		4 (450°C)	78	5	17	1.16	0.07
		2 (425°C)	68	4	28	0.51	0.03
IX	Z26(MoCO)	6 (500°C)	42	13	45	0.90	0.30
		6 (475°C)	27	5	68	0.60	0.11
		4 (450°C)	20	4	76	0.30	0.06
		3 (425°C)	14	2	84	0.16	0.02
X	Z26(MoAcac)	4 (500°C)	27	14	59	0.40	0.21
		2 (475°C)	25	23	52	0.19	0.17
		2 (450°C)	17	37	46	0.13	0.28
		1 (425°C)	13	47	40	0.05	0.17
XI	Z26(MoO_3)6%He	6 (500°C)	54	24	22	1.21	0.54
		3 (475°C)	35	30	35	0.39	0.33
		2 (450°C)	23	41	36	0.17	0.31
		1 (425°C)	12	25	63	0.04	0.09
XII	BEA(MoO_3)	8 (500°C)	35	27	38	1.00	0.80
		6 (475°C)	31	16	53	0.69	0.36
		5 (450°C)	29	8	63	0.54	0.15
		5 (425°C)	19	3	78	0.35	0.06
XIII	BEA(MoAcac)	9 (500°C)	47	19	34	1.60	0.60
		6 (475°C)	32	19	49	0.71	0.42
		4 (450°C)	24	8	69	0.36	0.12
		4 (425°C)	18	3	79	0.27	0.04
XIV	BEA(MoCO)	8 (500°C)	34	16	50	1.00	0.50
		7 (475°C)	30	8	62	0.78	0.21
		6 (450°C)	24	4	72	0.55	0.09
		4 (425°C)	19	3	79	0.28	0.04
XV	BEA($MoCl_5$)	5 (500°C)	39	4	57	0.70	0.10
		4 (475°C)	26	5	69	0.39	0.07
		5 (450°C)	20	4	76	0.37	0.07
		4 (425°C)	14	2	84	0.21	0.03
XVI	BEA($MoOCl_4$)	4 (500°C)	16	10	74	0.20	0.15
		4 (475°C)	9	6	85	0.13	0.09
		4 (450°C)	8	3	89	0.12	0.04
		4 (425°C)	6	1	93	0.09	0.01
XVII	BEA(Mo_7O_{24})	8 (500°C)	26	21	53	0.80	0.60
		6 (475°C)	23	21	56	0.51	0.47
		4 (450°C)	25	7	68	0.37	0.10
		4 (425°C)	24	2	74	0.36	0.03

Conditions: 0.2 g of catalyst, 10 % C_2H_6, 10 % NH_3, 10 % O_2, 70 % He. Contact time: 80 ms

Table S3: Catalytic behaviour of Mo containing solids in C_2H_4 ammoxidation at different temperatures

No	Catalyst	T (°C)	X (%)	S (%)		Ac_{CH_3CN} (μmol $s^{-1}g^{-1}$)
				CH_3CN	CO_2	
I	Mo–OFF	500	4	5	95	0.30
II	Mo–FER	500	4	11	89	0.70
III	Z26($MoCl_3$)	500	10	91	9	13.70
		475	6	86	14	7.75
		450	3	77	23	3.50
		425	2	50	50	1.50
IV	Z15($MoCl_3$)	500	9	84	16	11.40
		475	4	79	21	4.75
		450	2	60	40	1.80
		425	1	40	60	0.60
V	MOR($MoCl_3$)	500	5	63	37	4.73
		475	5	49	51	3.68
		450	5	25	75	1.88
		425	4	13	87	0.78
VI	BEA($MoCl_3$)	500	6	74	26	6.70
		475	3	60	40	2.70
		450	2	44	46	1.32
		425	1	22	78	0.33
VII	Z26($MoOCl_4$)	500	11	87	13	14.40
		475	9	39	61	5.27
		450	6	28	72	2.52
		425	4	16	82	0.96
VIII	Z26($MoCl_5$)	500	23	98	2	33.80
		475	12	93	7	16.74
		450	7	81	19	8.50
		425	4	79	21	4.75
IX	Z26(MoCO)	500	17	82	18	20.90
		475	12	67	33	12.06
		450	8	46	54	5.52
		425	4	39	61	2.34
X	Z26(MoAcac)	500	8	45	55	5.40
		475	6	39	61	3.51
		450	5	29	71	2.18
		425	4	19	81	1.14
XI	Z26(MoO_3)6%He	500	10	59	41	8.85
		475	7	45	55	4.73
		450	4	37	63	2.22
		425	2	19	81	0.57
XII	BEA(MoO_3)	500	14	92	8	19.30
		475	9	86	14	11.61
		450	6	81	19	7.30
		425	4	65	35	3.90
XIII	BEA(MoAcac)	500	13	93	7	18.10
		475	7	86	14	9.03
		450	4	74	26	4.44
		425	3	62	38	2.79
XIV	BEA(MoCO)	500	11	92	8	15.20
		475	6	86	14	7.74
		450	3	74	26	3.33
		425	2	60	40	1.80
XV	BEA($MoCl_5$)	500	9	68	32	9.20
		475	5	42	58	3.15
		450	5	29	71	2.18
		425	4	15	85	0.90
XVI	BEA($MoOCl_4$)	500	8	79	21	9.50
		475	6	57	43	5.13
		450	4	39	61	2.34
		425	2	25	75	0.75
XVII	BEA(Mo_7O_{24})	500	9	94	6	12.70
		475	6	89	11	8.00
		450	4	77	23	4.62
		425	3	61	39	2.75

Conditions: 0.05 g of catalyst, 10 % C_2H_4, 10 % NH_3, 10 % O_2, 70 %. Contact time: 20 ms

Table S4: Catalytic behaviour of the reference materials in C_2H_4 ammoxidation at different temperatures

No	Catalyst	T (°C)	X (%)	S (%)		Ac_{CH_3CN} (μmol $s^{-1}g^{-1}$)
				CH_3CN	CO_2	
XVIII	Z26(MoO_3)10%He	500	21	84	16	26.50
		475	11	48	52	7.92
		450	8	38	62	4.56
		425	6	19	81	1.71
XIX	Z140(MoO_3)6%He	500	5	74	26	5.60
		475	2	47	53	2.22
		450	1	41	59	0.62
		425	1	24	76	0.36
XX	Z15(MoO_3)Imp2%	500	11	91	9	15.00
		475	9	63	37	8.55
		450	7	34	66	3.57
XXI	Z15(MoO_3)Imp4%	500	20	99	1	29.50
		475	8	95	5	11.40
		450	5	95	5	7.13
		425	2	98	2	2.94
XXII	Z40(MoO_3)Imp2%	500	11	94	6	15.50
		475	8	88	12	10.56
		450	4	72	28	4.32
		425	2	53	47	1.59
XXIII	Z40(MoO_3)Imp4%	500	12	99	1	17.80
		475	6	95	5	8.55
		450	3	98	2	4.41
		425	1	98	2	1.47

Conditions: 0.05 g of catalyst, 10 % C_2H_4, 10 % NH_3, 10 % O_2, 70 %He. Contact time: 20 ms

Table S5: OFF and FER issued solids: Textural and chemical analyses results

Sample	S_{BET}/S_{micro} (m^2g^{-1})	V_p/V_{micro} ($cm^3\ g^{-1}$)	Si/Al			Mo/Al		
			ICP[a]	XPS[b]	EDX[b]	ICP[a]	XPS[b]	EDX[b]
H^+–OFF	5/–[**]	–/–[**]	3.34	–	–	–	–	–
NH_4^+–FER	–[**]	–[**]	9.11	–	–	–	–	–
Mo–OFF	108/103	0.05/0.05	3.44	0.50	3.57	0.32	4.00	0.33[*]
Mo–FER	–[**]	–[**]	8.77	0.50	–	0.48	8.50	–

[a] mol/mol, [b] atomic ratio

[*] Average value obtained from Table S6

[**] Value too low to be interpreted. According to Breck et *al*. (In Molecular Sieves, Chapter 29, 319–329. *Advances in Chemistry*, Volume 121, ACS Washington DC), the presence of cations in the exchange sites increases the density of nitrogen by 20 % over the normal liquid density (*i.e*. 0.95 g cm^{-3} as compared with 0.80 g cm^{-3} for liquid nitrogen at its boiling point). This value (0.95 g cm^{-3}) would correspond to the density of liquid nitrogen at a temperature of –227 °C. However, at this temperature, liquid nitrogen has a vapor pressure of 0.14 torr and the adsorbed nitrogen behaves as if its boiling point was 31°C below normal.

Table S6: EDX results obtained with Mo–OFF solid at four surface points
Chemical analysis of NH_4^+–FER, H^+–OFF, Mo–FER and Mo–OFF solids by ICP

Sample	Al (*wt*. %)	Si/Al (mol/mol)	Mo/Al (mol/mol)	Mo (*wt*.%)	Al *wt*. % (ICP)	Mo *wt*. % (ICP)
Mo–OFF	7.12	3.32	0.28	7.12	6.85	7.29
	6.04	3.77	0.34	7.23		
	6.22	3.22	0.38	8.45		
	6.41	3.98	0.30	6.87		
H^+–OFF	–	–	–	–	7.61	–
Mo–FER	–	–	–	–	3.43	5.87
NH_4^+–FER	–	–	–	–	3.72	–

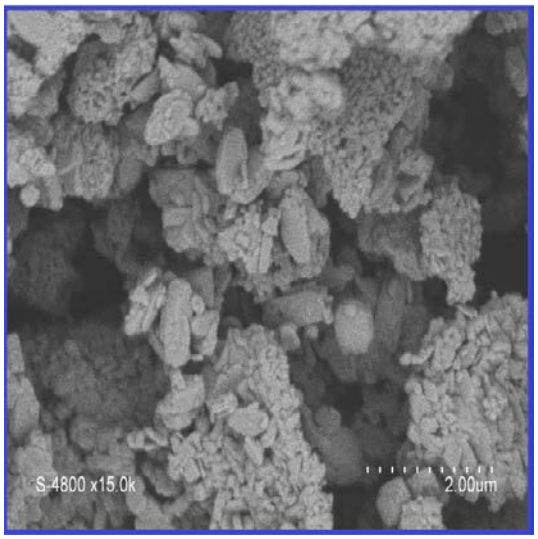

Fig. S1 Scanning electron microscopy micrograph of NH_4^+–FER sample

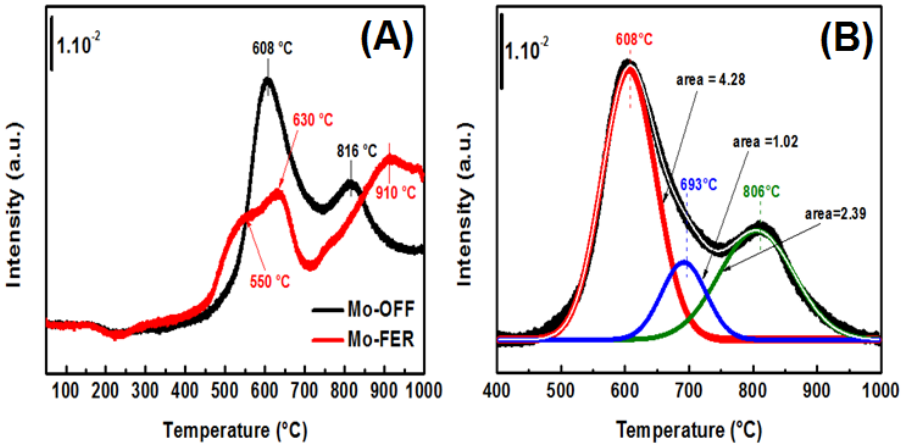

Fig. S2 (A) TPR profiles of Mo–OFF and Mo–FER solids, and **(B)** Deconvolution of the TPR profile of Mo–OFF solid. The reduction was performed with H_2(3 %)/Ar flow (30 cm^3 min^{-1}) using 70 mg of sample previously treated (in–situ) for 1 hour at 450 °C under air stream (30 cm^3 min^{-1}). Mo–FER solid was obtained by solid–state exchange of $MoCl_3$ into NH_4^+–OFF (9 *wt*. % Mo).
See Page S1 for more details about the techniques

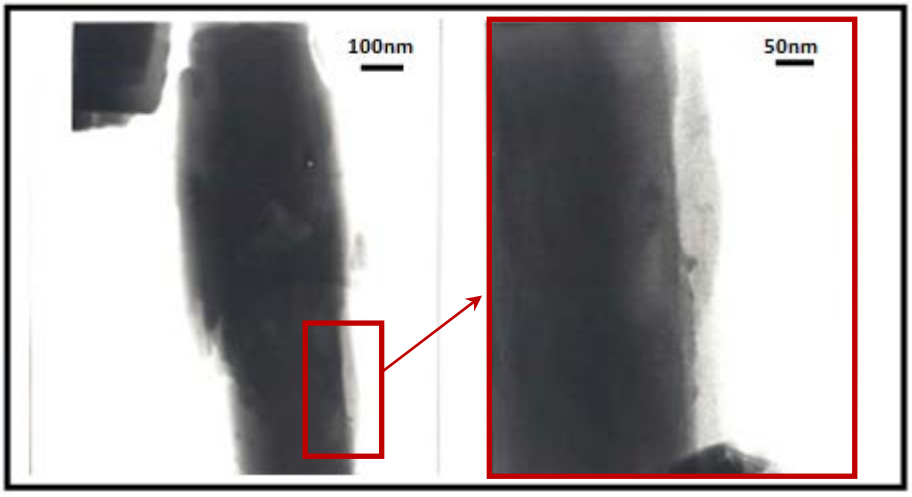

Fig. S3 TEM image of Mo–OFF solid. The sample was suspended and dispersed by ultrasonic treatment in acetone. A drop of the fine suspension was placed on a copper TEM grid, which was then loaded into the microscope

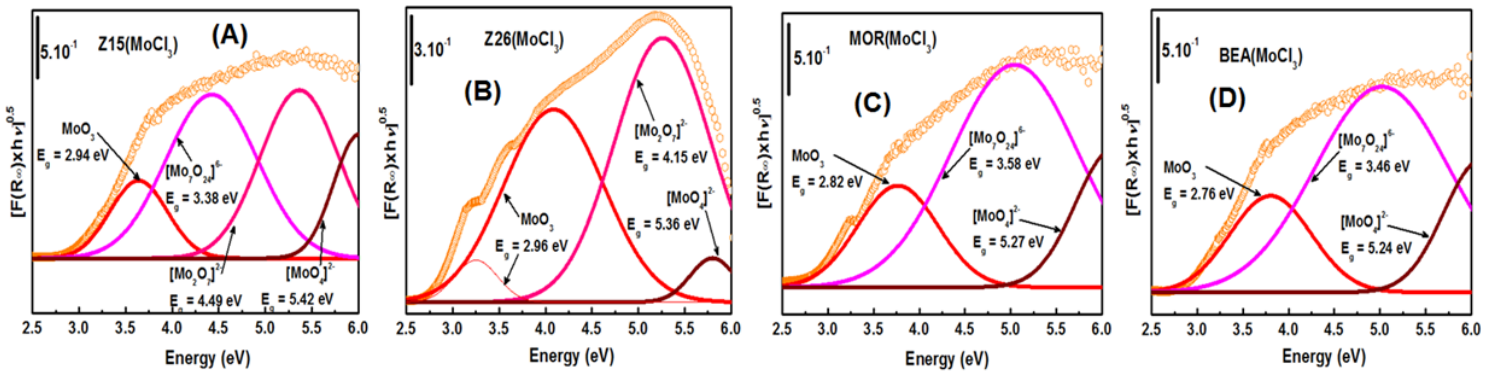

Fig. S4: Optical absorption spectrum of Z15($MoCl_3$), Z26($MoCl_3$), MOR($MoCl_3$) and BEA($MoCl_3$) solids. E_g: Edge energy value determined from the Schuster–Kubelka–Munk function (see Mannei et *al*. (2019) Chem Papers 73:619–633) for details)
Z15($MoCl_3$) solid was obtained by solid–state exchange of $MoCl_3$ into H^+–ZSM-5 (Si/Al = 15; 9 *wt*. % Mo)
Z26($MoCl_3$) solid was obtained by solid–state exchange of $MoCl_3$ into NH_4^+–ZSM-5 (Si/Al = 26; 6 *wt*. % Mo)
MOR ($MoCl_3$) solid was obtained by solid–state exchange of $MoCl_3$ into NH_4^+–MOR (9 *wt*. % Mo)
BEA($MoCl_3$) solid was obtained by solid–state exchange of $MoCl_3$ into NH_4^+–BEA (9 *wt*. % Mo)
See Page S1 for more details about the technique

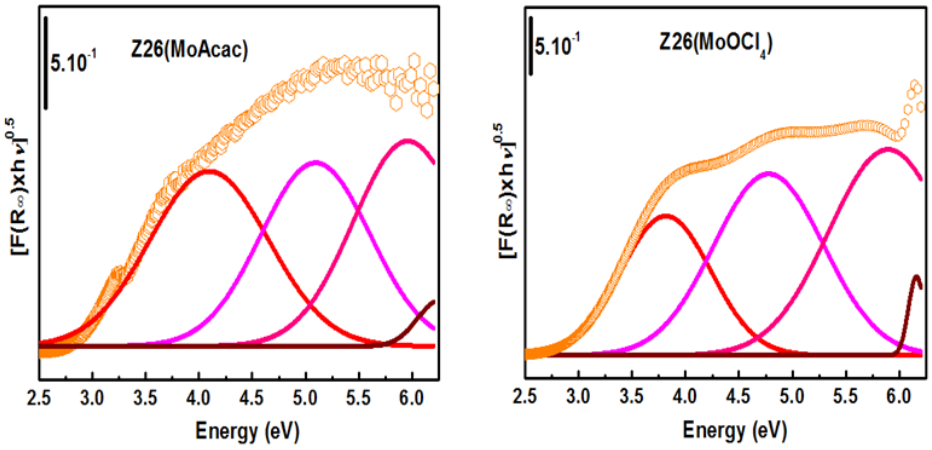

Fig. S5: Optical absorption spectra of Z26(MoAcac) and Z26($MoOCl_4$) solids. E_g: Edge energy value determined from the Schuster–Kubelka–Munk function (see Mannei et *al*. (2019) Chem Papers 73:619–633) for details)
See Fig. S4A for the attribution of each band
Z26(MoAcac) solid was obtained by solid–state exchange of $MoO_2(C_5H_7O_2)_2$ into NH_4^+–ZSM-5 (Si/Al = 26; 6 *wt*. % Mo)
Z26($MoOCl_4$) solid was obtained by solid–state exchange of $MoOCl_4$ into NH_4^+–ZSM-5 (Si/Al = 26; 6 *wt*. % Mo)
See Page S1 for more details about the technique

Table S7: NH_4^+–ZSM-5 (Si/Al = 26) issued solids: Edge energy (E_g) values relative to each Mo specie and the area of the corresponding band

	Edge energy (E_g) values (eV)/Area (*a.u.*)				
Sample	$[MoO_4]^{2-}$	$[Mo_2O_7]^{2-}$	$[Mo_7O_{24}]^{6-}$	MoO_3	Mo *wt.* % (EDX)
Z26($MoCl_5$)	–	4.20/2.45	–	2.85/1.87	3.06
Z26($MoCl_3$)	5.36/0.1268	4.15/1.65	–	2.96/1.36	4.90
Z26(MoCO)	–	4.72/2.33	3.81/1.74	2.96/1.50	3.00
Z26(MoO_3)6%He	5.56/N.D.	4.70/0.86	3.65/1.65	2.94/0.12	N.D.
Z26($MoOCl_4$)	5.97/0.1253	4.78/2.47	3.67/2.10	2.90/1.27	5.14
Z26(MoAcac)	5.83/0.1544	4.83/1.56	3.97/1.39	2.88/1.44	5.69

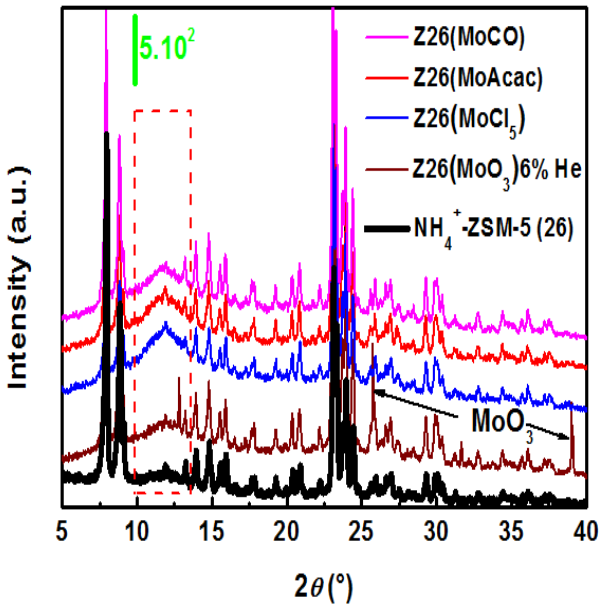

Fig. S6: XRD patterns of NH_4^+–ZSM-5 (Si/Al = 26) reference material and $Mo(CO)_6$, $MoO_2(C_5H_7O_2)_2$, $MoCl_5$ and MoO_3 issued solids: λ = 1.54060 Å, 40 kV, 40 mA, 0.2° min^{-1}

Table S8: Atomic and *wt.* % of Mo determined by EDX at five surface regions over the solid issued from NH_4^+–BEA and $(NH_4)_6Mo_7O_{24}{\cdot}4H_2O$ (6 *wt.* %) , *i. e.* BEA(Mo_7O_{24}) solid
BEA(Mo_7O_{24}) solid was prepared by solid–state exchange of $(NH_4)_6Mo_7O_{24}{\cdot}4H_2O$ into NH_4^+–BEA (6 *wt.* % Mo)

Spectrum	In stats.	O	Al	Si	Mo
Spectrum 1	Yes	70.52	2.25	26.72	0.51
Spectrum 2	Yes	71.38	2.26	26.18	0.18
Spectrum 3	Yes	68.82	2.32	28.61	0.25
Spectrum 4	Yes	70.21	2.27	27.36	0.16
Spectrum 5	Yes	74.26	1.85	22.89	1.00
Mean		71.04	2.19	26.35	0.42
Std. deviation		2.02	0.19	2.14	0.36
Max.		74.26	2.32	28.61	1.00
Min.		68.82	1.85	22.89	0.16

All results in atomic%

Spectrum	In stats.	O	Al	Si	Mo	Total
Spectrum 1	Yes	56.75	3.05	37.75	2.45	100.00
Spectrum 2	Yes	58.40	3.13	37.60	0.87	100.00
Spectrum 3	Yes	55.30	3.14	40.36	1.19	100.00
Spectrum 4	Yes	57.07	3.11	39.05	0.77	100.00
Spectrum 5	Yes	60.09	2.52	32.52	4.87	100.00
Mean		57.52	2.99	37.45	2.03	100.00
Std. deviation		1.81	0.26	2.98	1.73	
Max.		60.09	3.14	40.36	4.87	
Min.		55.30	2.52	32.52	0.77	

All results in weight%

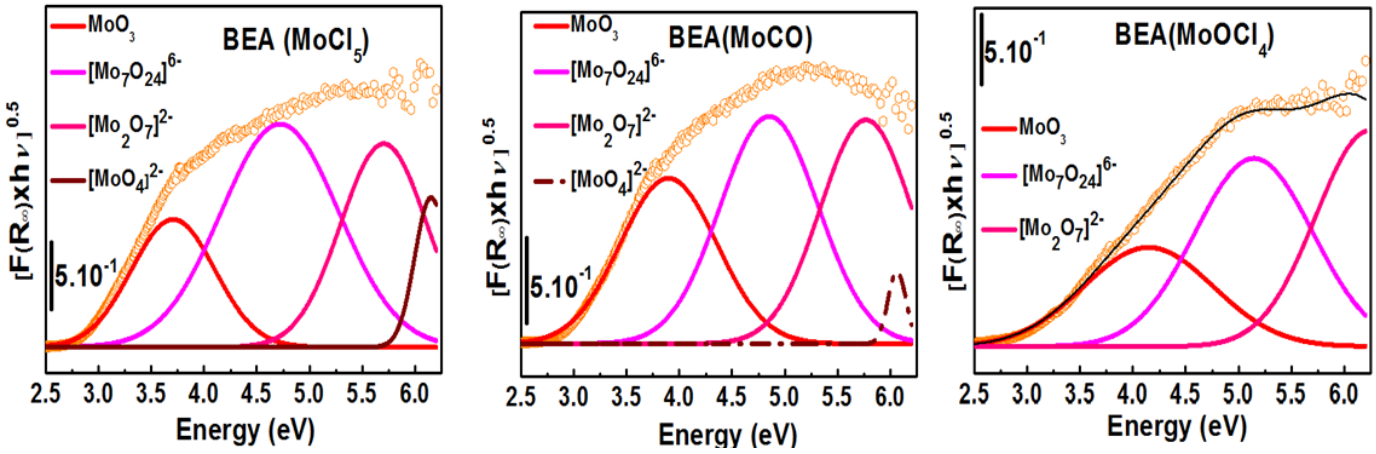

Fig. S7: Optical absorption spectra of Z26(MoAcac) and Z26($MoOCl_4$) solids. E_g: Edge energy value determined from the Schuster–Kubelka–Munk function (see Mannei et *al*. (2019) Chem Papers 73:619–633) for details)
See Fig. S4A for the attribution of each band
BEA($MoCl_5$) solid was obtained by solid–state exchange of $MoCl_5$ into NH_4^+–BEA (6 *wt.* % Mo)
BEA(MoCO) solid was obtained by solid–state exchange of $MoCO_6$ into NH_4^+–BEA (6 *wt.* % Mo)
BEA($MoOCl_4$) solid was obtained by solid–state exchange of $MoOCl_4$ into NH_4^+–BEA (6 *wt.* % Mo)
See Page S1 for more details about the technique

Table S9: NH_4^+–BEA issued solids: Edge energy (E_g) values relative to each Mo specie and the area of the corresponding band

	Edge energy (E_g) values (eV)/Area				
Sample	$[MoO_4]^{2-}$	$[Mo_2O_7]^{2-}$	$[Mo_7O_{24}]^{6-}$	MoO_3	Mo *wt.* % (EDX)
BEA($MoCl_3$)	5.24/1.20	–	3.46/3.25	2.76/0.95	6.14
BEA(MoO_3)	5.83/0.47	4.94/1.39	3.82/1.90	2.96/1.36	5.90
BEA(MoAcac)	–	4.84/1.74	3.59/2.21	2.75/1.15	6.07
BEA(MoCO)	5.86/0.09	4.83/1.47	3.87/1.62	2.90/1.15	5.09
BEA($MoCl_5$)	5.85/0.44	4.88/1.59	3.51/2.38	2.88/0.97	6.10
BEA($MoOCl_4$)	5.18/2.03	–	3.96/1.95	2.80/1.13	5.15

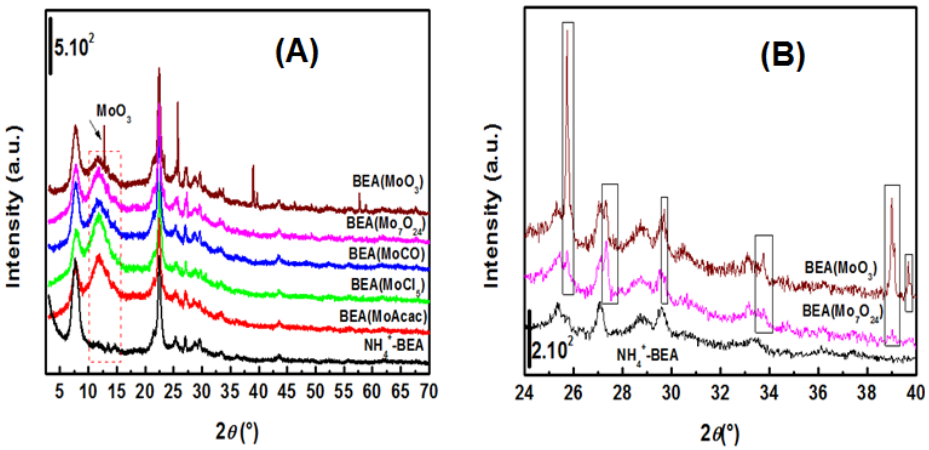

Fig. S8: XRD patterns of **(A)** NH_4^+–BEA zeolite and the issued solids, and **(B)** BEA(MoO_3), BEA(Mo_7O_{24}) solids and the corresponding support. Solid–square: crystalline MoO_3 diffraction lines (λ = 1.54060 Å, 40 kV, 40 mA, 0.2° min^{-1})

Table S10: TOF values obtained in ethane ammoxidation over NH_4^+–ZSM-5 (Si/Al=26) and NH_4^+–BEA issued solids between 425 and 500 °C

	TOF (/s)	TOF (/h)	TOF (/s)	TOF (/h)	TOF (/s)	TOF (/h)	TOF (/s)	TOF (/h)	TOF (/s)	TOF (/h)	TOF (/s)	TOF (/h)
	Z26MoCl5	Z26MoCl5	Z26MoOCl4	Z26MoOCl4	Z26MoCl3	Z26MoCl3	Z26MoCO	Z26MoCO	Z26MoO3	Z26MoO3	Z26MoAcac	Z26MoAcac
500	0,03802281	136,882129	0,00375	13,5	0,02415094	86,9433962	0,01253333	45,12	0,04321429	155,571429	0,008	28,8
475	0,0234474	84,4106464	0,0035	12,6	0,0045283	16,3018868	0,008	28,8	0,00607143	21,8571429	0,0038	13,68
450	0,01470215	52,9277567	0,00225	8,1	0,00245283	8,83018868	0,004	14,4	0,00607143	21,8571429	0,0026	9,36
425	0,00646388	23,269962	0,0015	5,4	0,00188679	6,79245283	0,00213333	7,68	0,00142857	5,14285714	0,001	3,6

	TOF (/s)	TOF (/h)	TOF (/s)	TOF (/h)	TOF (/s)	TOF (/h)	TOF (/s)	TOF (/h)	TOF (/s)	TOF (/h)	TOF (/s)	TOF (/h)
	BEAMoCl5	BEAMoCl5	BEA(MoOCl4	BEA(MoOCl4	BEAMoCl3	BEAMoCl3	BEA(MoCO)	BEA(MoCO)	BEA(MoO3)	BEA(MoO3)	BEA(MoAcac	BEA(MoAcac
500	0,00503448	18,1241379	0,00237624	8,55445545			0,00179104	6,44776119	0,00818898	29,480315	0,00987421	35,5471698
475	0,00268966	9,68275862	0,00128713	4,63366337			0,00097015	3,49253731	0,00543307	19,5590551	0,00446541	16,0754717
450	0,00255172	9,1862069	0,00118812	4,27722772			0,00089552	3,2238806	0,00425197	15,3070866	0,00226415	8,1509434
425	0,00144828	5,2137931	0,00089109	3,20792079			0,00067164	2,41791045	0,00275591	9,92125984	0,00169811	6,11320755

Table S11: TOF values obtained in ethylene ammoxidation over NH_4^+–ZSM-5 (Si/Al=26) and NH_4^+–BEA issued solids between 425 and 500 °C

	TOF (/s)	TOF (/h)	TOF (/s)	TOF (/h)	TOF (/s)	TOF (/h)	TOF (/s)	TOF (/h)	TOF (/s)	TOF (/h)	TOF (/s)	TOF (/h)
	Z26MoCl5	Z26MoCl5	Z26MoOCl4	Z26MoOCl4	Z26MoCl3	Z26MoCl3	Z26MoCO	Z26MoCO	Z26MoO3	Z26MoO3	Z26MoAcac	Z26MoAcac
500	0,42851711	1542,6616	0,1795	646,2	0,25754717	927,169811	0,2788	1003,68	0,31607143	1137,85714	0,108	388,8
475	0,2121673	763,802281	0,065875	237,15	0,14622642	526,415094	0,1608	578,88	0,07928571	285,428571	0,0702	252,72
450	0,10773131	387,8327	0,0315	113,4	0,06603774	237,735849	0,0736	264,96	0,07928571	285,428571	0,0436	156,96
425	0,06020279	216,730038	0,012	43,2	0,02830189	101,886792	0,0312	112,32	0,02035714	73,2857143	0,0228	82,08

	TOF (/s)	TOF (/h)	TOF (/s)	TOF (/h)	TOF (/s)	TOF (/h)	TOF (/s)	TOF (/h)	TOF (/s)	TOF (/h)	TOF (/s)	TOF (/h)
	BEAMoCl5	BEAMoCl5	BEA(MoOCl4	BEA(MoOCl4	BEAMoCl3	BEAMoCl3	BEA(MoCO)	BEA(MoCO)	BEA(MoO3)	BEA(MoO3)	BEA(MoAcac	BEA(MoAcac)
500	0,06331034	227,917241	0,02633333	94,8			0,07074627	254,686567	0,15212598	547,653543	0,11408805	410,716981
475	0,02172414	78,2068966	0,01425	51,3			0,03828358	137,820896	0,09141732	329,102362	0,05679245	204,45283
450	0,01503448	54,1241379	0,0065	23,4			0,01746269	62,8656716	0,05748031	206,929134	0,02792453	100,528302
425	0,0062069	22,3448276	0,00208333	7,5			0,00559701	20,1492537	0,03070866	110,551181	0,01754717	63,1698113

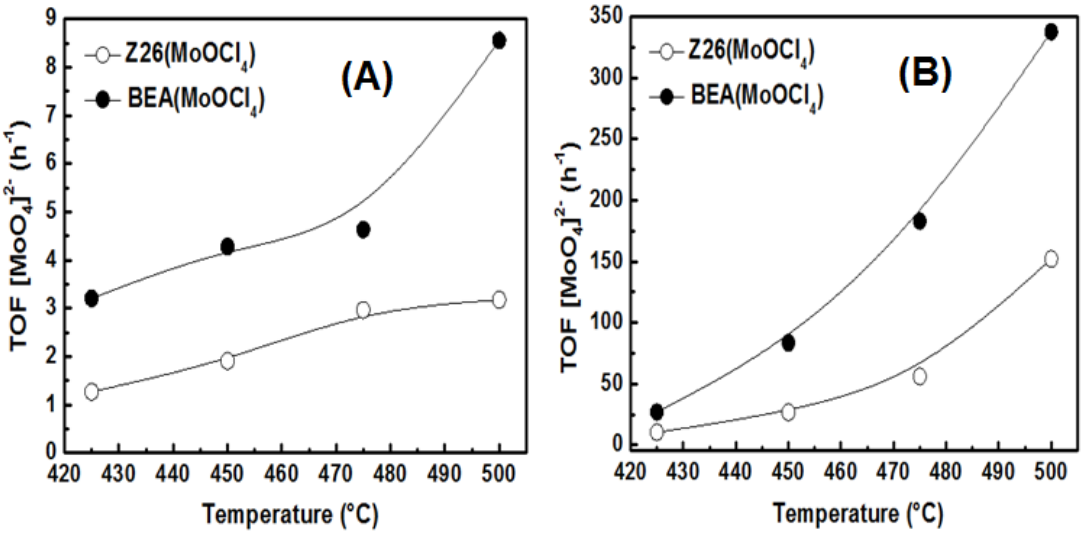

Fig. S9: (A) Ethane, and **(B)** ethylene ammoxidation over NH_4^+–BEA issued solids: TOF values relative to $[MoO_4]^{2-}$ species for acetonitrile activity as a function of reaction temperature (see Tables S10 and S11 for values)
For ethane ammoxidation: 0.2 g of catalyst, 10 % C_2H_6, 10 % NH_3, 10 % O_2, 70 % He. For ethylene ammoxidation: 0.05 g of catalyst, 10 % C_2H_4, 10 % NH_3, 10 % O_2, 70 % He

Characterization of reference materials

The textural properties of selected reference materials are illustrated herein:

Textural properties of selected reference materials

Sample	S_{BET}/S_{micro} (m^2g^{-1})	V_p/V_{micro} ($cm^3\ g^{-1}$)
NH_4^+–ZSM-5 (26)	367/291	0.21/0.13
Z26(MoO_3)6%O_2	250/165	0.15/0.08
Z140(MoO_3)6%He	330/190	0.20/0.09
Z140(MoO_3)6%O_2	329/100	0.19/0.05
H^+–ZSM-5 (15)	362/292	0.22/0.13
Z15(MoO_3)Imp2%	354/227	0.24/0.10

If we compare the textural properties of Z140(MoO_3)6%He and Z140(MoO_3)6%O_2 solids, we notice similar S_{BET} values but the later solid exhibited the lowest microporous area and volume (0.05 $cm^3\ g^{-1}$). Apparently, the oxidative treatment encourages the diffusion of Mo inside the internal cavities of NH_4^+–ZSM-5 (Si/Al = 140) zeolite. However, in the case of the impregnated solid (*i.e.* Z15(MoO_3)Imp2%), the internal area of H^+–ZSM-5 zeolite (Si/Al =15) deceases despite the use of low Mo amount (2 *wt.* %).

The textural properties of Z26(MoO_3)6%He (Table 3 in the manuscript) and Z26(MoO_3)6%O_2 (Table 7 in the manuscript) solids indicate that the oxidative treatment decreases the microporous area and the (micro)porous volume(s) of NH_4^+–ZSM-5 (Si/Al =26). According to XRD results compiled in Fig. S10A–C, the intensity of MoO_3 diffraction lines over Z26(MoO_3)6%O_2 solid is lower if compared with those of Z26(MoO_3)6%He, evidencing that MoO_3 oxide diffuses throughout the zeolite micropores. Nevertheless, the use of 10 *wt.* % Mo in Z26(MoO_3)10%He solid favoured the formation of crystalline MoO_3 as revealed by the increase in the corresponding diffraction lines.

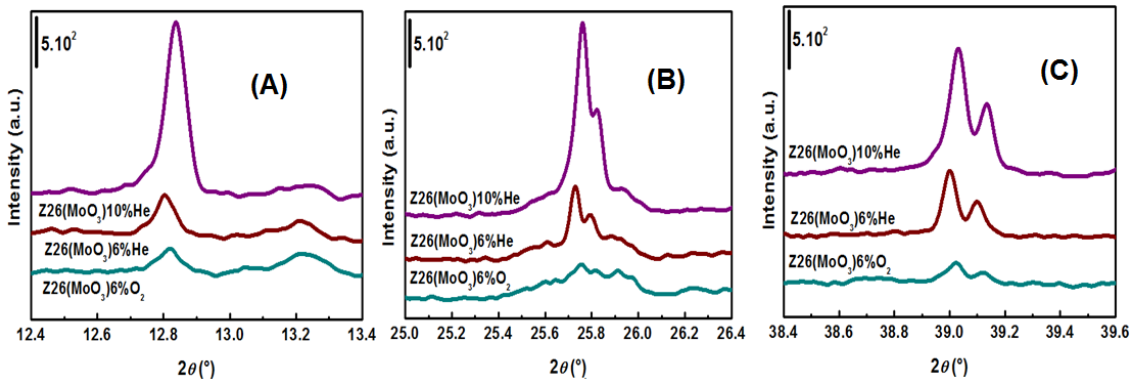

Fig. S10: XRD profiles of Z26(MoO_3)6%O_2, Z26(MoO_3)6%He and Z26(MoO_3)10%He solids. Diffraction lines of crystalline MoO_3 which correspond to **(A)** (020) plane, **(B)** (040) plane, and **(C)** (060) plane
λ = 1.54060 Å, 40 kV, 40 mA, 0.2° min^{-1}
The three solids were prepared by solid–state exchange of MoO_3 (6 and 10 *wt*. % Mo) into NH_4^+–ZSM-5, (Si/Al =26) under the appropriate carrier gas

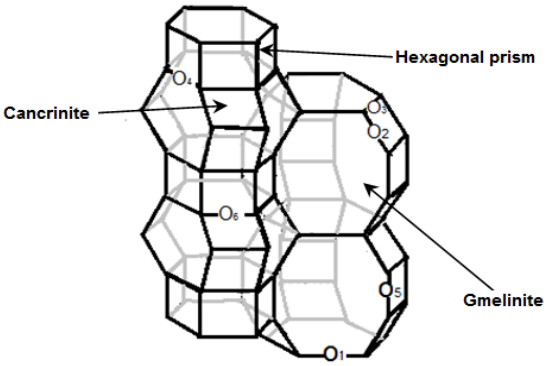

Scheme S1 Offretite structure and oxygen atoms numbered according to Mirodatos et *al*. (J Chem Soc, Faraday Trans 1 74:1786–1795): O_1, O_2, O_4 and O_5 oxygen atoms are shared between the cages and the channel. O_2 and O_4 atoms are in the cancrinite cage, O_6 in the hexagonal prism and O_5 in the channel